Chemical Papers (2022) 76:7061–7073
https://doi.org/10.1007/s11696-022-02373-z

ORIGINAL PAPER

An efficient 2-aminothiazolesalicylaldehyde fluorescent chemosensor for Fe^{2+} ion detection and a potential inhibitor of NUDT5 signaling hormone for breast cancer cell and molecular keypad lock application

Summaya Banu Basha[1] · Immanuel David Charles[2] · Nandhakumar Raju[2] · Sakthivel Manokaran[3] · Hemalatha Kuzhandaivel[1]

Received: 25 February 2022 / Accepted: 12 July 2022 / Published online: 4 August 2022

Abstract

A novel thiazole phenol conjugate, 2-aminothiazolesalicylaldehyde (receptor1) was designed and synthesized for the first time through a single step process via Schiff base condensation reaction. The formation of receptor1 was confirmed by FTIR, ^{13}C NMR, and ^{1}H NMR. The IR spectra confirmed the presence of the aldimine formation. It is further supported by the proton NMR, showing the disappearance of aldehyde peaks and the formation of a new imine peak. This is further corroborated by the ^{13}C NMR. The receptor1 complexing with various metal ions were studied through fluorescence spectroscopy showed its selectivity toward Fe^{2+} ion following a reverse photoinduced electron transfer (PET) process compared to all other potentially competing ions. The receptor1 was applied as a sensor to sense Fe^{2+} ion in water samples. The detection limit for Fe^{2+} ion in drinking water was substantially lower (0.003 μM) than the EPA (environmental protection agency) recommendation (5.37 M). The capability of receptor1 in recovering Fe^{2+} ion in bore water, tap water, and drinking water was up to 99.5%. The receptor1 was also used as a chelating ligand (receptor1) in molecular docking and it was assessed as a potential inhibitor of NUDT5, a silence hormone signaling for breast cancer. The test compound (PDB: 5NWH) showed good affinity toward the target receptor1 with the binding energy of – 5.23 kcal mol^{-1}. Furthermore, the receptor1 showed excellent reversibility property on adding EDTA solution. Due to the marvelous reversible property, a molecular-scale sequential information processing circuit is designed for the multi-task behavior such as 'Writing-Reading-Erasing-Reading' in the form of binary logic gate. The consecutive addition of Fe^{2+} ion and EDTA solution to receptor1 paves a way for the construction of INHIBIT logic gate. Additionally, the receptor1 showed the mimicking behavior of molecular keypad lock.

Keywords Salicylaldehyde · Reverse PET · Fluorescent quenching · Molecular docking · NUDT5

Introduction

The fluorometric studies have great impact on the detection of metal ion in the biological and environmental system in recent years (Khairnar et al. 2015). Iron is the most abundant metal found in the earth's crust next to aluminum. It is a major mineral required for the human body for the development of the immune system, synthesis of hemoglobin, and transfer of electrons in the photophysical process (Jo 2017; Tamil Selvan 2018; Kim 2013; Jo 2013; Bhuvanesh 2017). Due to its significant catalytic property, iron is used as a catalyst in numerous reactions such as DNA and RNA synthesis, enzyme catalysis, and cellular metabolism (Lee et al. 2012). Intake of excess iron may cause neurodegeneration such as Parkinson's disease, Alzheimer's, Huntington's, and Menke's diseases (Li et al. 2016). Iron deficiency

✉ Nandhakumar Raju
nandhakumar@karunya.edu

✉ Hemalatha Kuzhandaivel
hemalatha.kv@cit.edu.in

[1] Department of Chemistry, Coimbatore Institute of Technology, Anna University, Coimbatore 641 014, India

[2] Department of Chemistry, Karunya Institute of Technology and Sciences, KarunyaNagar, Coimbatore 641114, India

[3] Department of Bioinformatics, Intergrated Bio Computing Laboratory, Bharathiar University, Coimbatore 641046, India

weakens the immune system, allowing lethal viruses such as pneumonia, typhoid, COVID-19, and others to enter the body. Liver damage, diabetes, anemia, kidney damage and heart disease are all possible side effects of iron deficiency. (Chereddy 2013; Xu 2017; Murugan 2018; Joseph 2011; Gong 2019). In the biological system, the distinction between ferric and ferrous ion is rather difficult in the detection process of iron (Zhan 2012; Yoldas 2015; Farhi 2018; Wang 2016; Yin 2011; Sen 2012; Moon 2010; Dong 2010; Asiri 2019), the Schiff-based compound like 2-aminothiazolesalicylaldehyde plays a major role in detecting the ferric ion in particular. In the Schiff-based compound, the presence of a π-conjugated aromatic chromogenic group helps to sense cation and anion molecules (Zhang et al. 2020). Among the entire heterocyclic group, the sulfur-containing thiazole group has the greatest impact in the medicinal field due to its anti-cancer, anti-tubercular, and antimicrobial properties (Balasubramanian et al. 2020). For the past few years, biosensor, chromogenic sensors, mass sensors, and the electrochemical sensor were reported for sensing toxic metals in the environment (Gholami et al. 2015). Among these techniques, the fluorescent chemosensor method is highly efficient due to its specific selectivity of ion, responds for both solid and liquid phases, responds for a short time and is cost-efficient (Huang et al. 2012). As per literature review, Golbedaghi et al. have reported 81% yield of salicylaldehyde (2-[3-(2-formyl phenoxy)propoxy]benzaldehyde-2-aminobenzenethiol) Schiff-based compound. The compound sensed Fe^{3+} ion in H_2O-DMF solution (Golbedaghi et al. 2018). Li et al. reported salicylaldehyde (4-N,N-diethylaminosalicylaldehyde hydrazone) Schiff-based chemosensor with the yield of 57% for specific detection of Zn^{2+} ion (Li et al. 2010). Chao Gou et al. have reported 75% yield of salicylaldehyde (4- hydroxysalicylaldhyde-hydrazine) bis Schiff-based chemosensor for selective detection of Cu^{2+} and Al^{3+} ion (Chao Gou et al. 2011). In this article, 2-aminothiazolesalicylaldehyde (receptor1) was synthesized by conjugating thiazole with salicylcaldehyde to form C = N imine based Schiff-based compound with the yield of 88%, which showed fluorescence quenching with Fe^{2+} ion through a probable reverse photoinduced electron transfer (PET) process. Various studies conducted on Schiff-based compound showed the limit of detection of Fe^{2+} ion to be 0.32 µM (Tae Geun Jo), 1.09 µM (Atikal Farhi), 1.3 µM (Kyung Beom Kim), 0.0048 µM (Bhuvanesh), and so on. This is the first time that the Schiff-based compound detected the Fe^{2+} metal ion at a very low concentration of 0.0033 µM. The 2-aminothiazolesalicylaldehyde showed an excellent reversibility property (turn on–off–on–off) with EDTA. The reversible property of Schiff base is applied for the establishment of INHIBIT molecular logic gate and molecular keypad lock. The receptor1 was subjected to the detection of Fe^{2+} ion in real water sample analysis using fluorescence technique. The synthesized receptor1 was assessed for its ability to interact with protein receptor through molecular docking, which is an important tool for drug discovery. The receptor1 was docked with NUDT5 (PDB ID: 5NWH) which is a hormone, signaling for breast cancer cells.

Experimental

Materials and instruments

Grade quality solvents and reagents were purchased commercially. Highly purified compound such as 2-aminothiazole and salicylaldehyde was purchased from Hi-media. The ^1H and ^{13}C NMR spectra were recorded from Bruker 400 and 100 MHz spectrometer using DMSO-d_6 solvent and Trimethylsilane (TMS) as an internal standard. Absorption studies were carried out using Shimadzu UV-240 spectrophotometer. The fluorescence study was recorded on Jasco FP-8200 spectrofluorometer. The absorption and emission spectra were recorded at 24 ± 1 °C.

Synthesis of 2-aminothiazolesalicylaldehyde

Salicylaldehyde (0.5 mL, 1 mmol) was dissolved in 30 mL of methanol, and then 2-aminothiazole (200 mg, 1 mmol) was added. About 3–4 mL glacial acetic acid was added to this mixture and stirred constantly for 17 h at room temperature (Zhou et al. 2011). Thin-layer chromatography was used to examine the product formation as a preliminary test. The solvent evaporation was detected after a few days, along with an oily brownish-yellow coating at the top of the reaction mixture, and the reaction mixture eventually transformed into a brownish-yellow colored chemical. FTIR, ^{13}CNMR, and ^1H NMR were used to validate the synthesis of 2-aminothiazolesalicylaldehyde (Scheme 1), which was given the name receptor1. The yield of the synthesized product is 88%.

UV–Vis absorption studies

UV–Vis absorption tests were conducted to determine the excitation wavelength for the synthesized receptor1 and, as a result, to analyze the photophysical characteristic by fluorescence investigations. Receptor1 (2 mg) was dissolved in 5 mL of DMF (dimethylformamide) at a concentration of 2×10^{-3} M to make the stock solution. To keep the pH constant, 50 mM of HEPES (4-(2-hydroxyethyl)-1-piperazineethanesulfonic acid) buffer was dissolved in DMF and H_2O at a ratio of 1:1 (Saravanan et al. 2019). To observe the change in absorbance, a concentrated solution of 2×10^{-5} M and 2×10^{-6} was produced from the stock solution. The experiment was carried out at a pH of 7.4 (neutral).

Scheme 1 Synthesis of receptor1 (2-aminothiazolesalicylaldehyde)

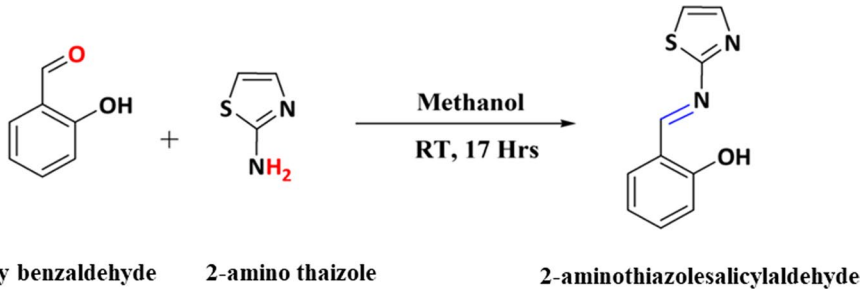

2-Hydroxy benzaldehyde 2-amino thaizole 2-aminothiazolesalicylaldehyde

Fluorescence titration

To conduct the fluorescence titration, a stock solution of receptor1 at a concentration of 4×10^{-6} M was produced (2 mg, 0.01 mmol). Metal nitrate salts of Ag^{+}, Zn^{2+}, Fe^{2+}, Fe^{3+},K^{+}, Li^{+}, Na^{+} (1 mg, 0.01 mmol)) Ba^{2+}, Ca^{2+}, Co^{2+}, Cu^{2+},Ni^{2+}, Sr^{2+} (2 mg,0.01 mmol) Al^{3+},Pb^{2+}, Hg^{2+},Zr^{2+}, Mg^{2+}, Mn^{2+} (3 mg, 0.01 mmol) Bi^{3+}, Cr^{3+} (4 mg, 0.01 mol), and Cd^{2+} (7 mg, 0.01 mol) were weighed and dissolved in 25 mL DMF–H_2O, 1:1 v/v, HEPES 50 mM buffer solution (Prabhu et al. 2015a, b). To make 100 equivalents, 2 mL of metal solution was mixed to 2 mL of receptor1. At an excitation wavelength of (λ_{ex}) 275 nm, the fluorescence intensity of each metal bound to receptor1 was measured.

Competition with other metal ions

The interference of other metal ions during the sensing of Fe^{2+}using receptor1 was investigated by including 100 equivalents of each metal salt (0.01 mmol) (M = Ag^{+}, Al^{3+}, Ba^{2+}, Bi^{3+}, Ca^{2+}, Cd^{2+}, Co^{2+}, Cr^{3+},Cu^{2+}, Fe^{3+}, Hg^{2+}, K^{+}, Li^{+},Mg^{2+}, Mn^{2+}, Na^{+}, Ni^{2+}, Pb^{2+}, Sr^{2+}, Zr^{2+}, and Zn^{2+}) (Nagarajan et al. 2021) dissolving in buffer solution. At the excited wavelength (λ_{ex}) 275 nm, the fluorescence intensity was measured. Two mL of receptor1 and 2 mL of each metallic solution were added to each vial, and fluorescence was measured. To test the interference behavior, 2 mL of Fe^{2+} ion solution was added to each vial.

Job's plot measurements.

To assess the stoichiometry of the receptor1–Fe^{2+} complex equal concentration of receptor1 (host) and Fe^{2+} (guest) of strength 1×10^{-6} M was prepared. The receptor1 and the metal ion solution were mixed at the ratio of 0:4, 0.1:3.9, 0.2:3.8, 0.3:3.7, 0.4:3.6, 0.5:3.5, 0.6:3.4, 0.7:3.3, 0.8:3.2, 0.9:3.1, and 1:3 mL. The fluorescence analysis was carried out by transferring 4 mL of the above solution to the cuvette. The binding stoichiometric was evaluated using the Jobs plot (Suresh et al. 2018) and the nonlinear fitting curve.

Quantum yield measurement

The quantum yield (ϕ) was calculated using quinine sulfate ($\phi_R = 0.54$) as a standard, the equation for calculating quantum yield (Kumar 2020; Chae 2019) is

$$\Phi_U = \Phi_R \times F_U/F_S \times A_S/A_U \times \eta_U^2/\eta_S^2 \quad (1)$$

where ϕ_R is a standard value (Quinine Sulfate), F_U and F_S are the integrated fluorescence intensity of unknown and standard sample, A_S and A_U are the absorbance of the standard and unknown sample, $\eta_U{}^2$ is the refractive index of solvent in which unknown sample was dissolved (1.4305), and $\eta_S{}^2$ is the refractive index of solvent in which standard was dissolved (1.33) (Khan et al. 2021). The quantum yield of receptor1 (ϕ_U) is 0.0126 and for receptor1–Fe^{2+} is 0.0036 at 275 nm.

Docking parameters

Molecular docking plays a vital role in drug discovery. It is a useful platform for predicting the protein ligand interaction through binding mechanism. The structure of the protein–ligand was accomplished using Schrodinger maestro software. Structure of the Schiff bases was sketched using 2D chemsketch. The active site residue information was collected from PDB (Protein Data Base) sum entry. In receptor-grid generation, a 10 × 10 x 10 Å receptor grid box was generated around the active site residues of target protein. The docking study exposes the most suitable binding sites in the target protein for the ligand to bind.

Results and discussion

Design and synthesis of 2-aminothiazolesalicylaldehyde

Receptor1 was synthesized by condensation of 2-Hydroxy benzaldehyde and 2-amino thiazole in methanol with 88% yield as shown in Scheme 1 and characterized by ^{1}H-NMR

and ^{13} C-NMR. In receptor1 benzaldehyde, the group acts as a fluorophore, the imine group acts as a spacer, and the heterocyclic thiazole group containing N and S atom acts as a binder. The imine group links the fluorophore and binding unit. From FTIR analysis, the presence of skeletal stretching of the aromatic group is confirmed from the peak at 1600.92 cm^{-1}, the peak at 1192.21 cm^{-1} showed C–O stretching vibration of alcohol, the peak at 1492.00 cm^{-1} confirms C–C stretching vibration, the peak at 756.00 cm^{-1} confirms C–S stretching vibration, and the peak at 2742.78 cm^{-1} confirms C-H stretching vibration. The peak at 1658.78 cm^{-1} confirms the presence of the C = N stretching band (Fig. S1) (Ahmed et al. 2015). The total number of carbon was confirmed by ^{13}C NMR. The chemical shift was noticed at (100 MHz, DMSO: d6, ppm) 130.14, 122.72, 128.32, 117.70, 154.62, 128.53, 140.48, 139.36, 128.96, 129.07. The total number of hydrogen was confirmed by ^{1}H NMR. The chemical shift of H^1 NMR (400 MHz, DMSO: d_6, δ, ppm) (*J*, Hz): 7.01, 7.12, 7.15 and 7.17 (d, 4H, Ar–H), 6.94 (s, 1H, CH = N), 6.85 and 6.94 (d, 2H, CH_2), and 9.23 (s, 1H, 1-OH) (Fig. S2 and S3) (Kim et al. 2020) was observed. Analytically calculated mass value for $C_{10}H_8N_2SO$ (204.23): C, 120.10; H, 8.06; N, 28.01.

Selectivity studies

The selectivity studies are performed to assess the sensing behavior of receptor1 for selective detection of the metal ion. The metal ions such as Ag^+, Al^{3+}, Ba^{2+}, Bi^{3+}, Ca^{2+}, Cd^{2+}, Co^{2+}, Cr^{3+},Cu^{2+}, Fe^{2+}, Fe^{3+}, Hg^{2+}, K^+, Li^+, Mg^{2+}, Mn^{2+}, Na^+, Ni^{2+}, Pb^{2+}, Sr^{2+}, Zr^{2+}, and Zn^{2+} are taken in the form of nitrate salts and added to receptor1 and buffer solution. The excitation wavelength is fixed as 275 nm from UV–Vis spectroscopy. The receptor1 responded to a drastic quenching effect with Fe^{2+} and Ag^+ ions as shown in (Fig. 1). However, other metal ions showed no significant changes during the identical condition. As a result, the receptor1 showed a potential response for Fe^{2+} ion with a turn on–off fluorescence through a possible reverse PET mechanism.

Proposed binding mechanism

In PET-based sensors, a fluorophore is usually connected via a spacer to a binding unit containing a relatively high energy non-bonding electron pair found in nitrogen donors, capable of transferring an electron to the excited fluorophore to quench its fluorescence (off–on) (Golbedaghi et al. 2018). The quenching takes place because of the deactivation of the excited state of the fluorophore by the addition of an electron to its excited state frontier orbitals from the functional group of the fluorophore that quenches the fluorescence intramolecularly (Li et al. 2009). This leads to the non-emissive state of a fluorophore. Here,

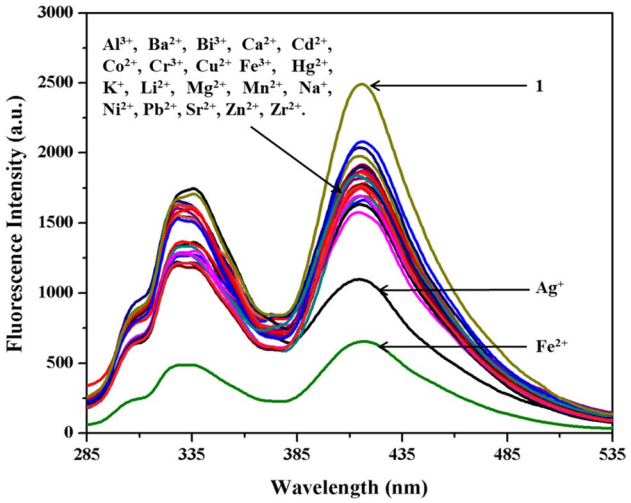

Fig. 1 Fluorescence spectra to assess the response of various metal ion (100 equivalents. of each, λ_{ex} = 275 nm) toward receptor1 of concentration $4 \times 10.^{-6}$ M solution (DMF–H_2O, 1:1 v/v, HEPES 50 mM, pH = 7.4)

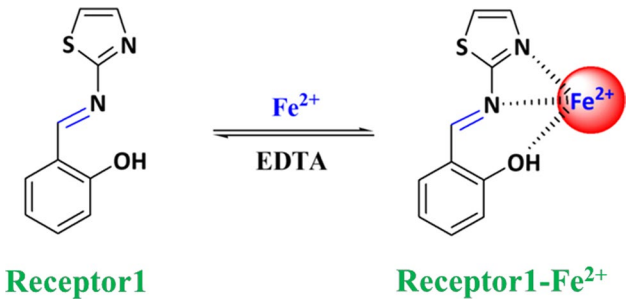

Scheme 2 Proposed binding mechanism

in receptor1 the free electron pair of nitrogen present in thiazole and C = N group attached to the fluorophore has strong fluorescence emission, and binding of cation results in weak fluorescence emission because the Fe^{2+} ion bound to receptor1 is paramagnetic with unfilled d-subshell that strongly quench the fluorescence intensity of the fluorophore through electron transfer between receptor1 and Fe^{2+} ion (Gou et al. 2011). The Fe^{2+} ion bound to the fluorophore acts as a signal transduction unit and is also bound with a thiazole moiety and spacer (Das et al. 2013). There is no possibility of Fe^{2+} ion binding with sulfur because of the weak interaction between Fe^{2+} and sulfur (Fan et al. 2014). Therefore, the quenching response of receptor1 toward Fe^{2+} ascribed to electrons of fluorophore transferring to the binding unit by metal ion complexation (reverse-PET process), resulting in fluorescence quenching (Scheme 2) (Luo et al. 2016). Additionally, the ESIPT mechanism takes place between the proton donating hydroxyl group and withdrawing imine group upon

excitation of a molecule via intramolecular hydrogen bond formation.

Interference study

An interference study was carried out to predict if any competitive metal ion interferes during the complexation of receptor1 with Fe^{2+}. Figure 2 shows a change in the fluorescence intensity for the addition of metal ions to receptor1. The emission intensity of receptor1 with various metal ion such as Al^{3+}, Ba^{2+}, Bi^{3+}, Ca^{2+}, Cd^{2+}, Co^{2+}, Cr^{3+},Cu^{2+}, Fe^{3+}, Hg^{2+}, K^{+}, Li^{+}, Mg^{2+}, Mn^{2+}, Na^{+}, Ni^{2+}, Pb^{2+}, Sr^{2+}, Zr^{2+}, and Zn^{2+} is on par to the emission intensity of receptor1 alone, whereas the emission intensity of receptor1–Ag^{+} is low compared to the emission intensity of other receptor1–metal ion complex. This is due to the fact that the electronic configuration of the Ag^{+} ion in the 4d subshell is filled, resulting in diamagnetic property, which causes a drop in emission intensity since no electron transfer occurs between Ag^{+} and receptor1. The HSAB (Hard-Soft and Acid–Base) theory predicts that the borderline base (C = N) group can coordinate with a borderline acid Fe^{2+} ion in receptor1's response to Fe^{2+} (Ahmed Nuri Kursunlu 2015; Li 2018). The reverse PET mechanism caused the fluorescence intensity of receptor1 to decrease when it was complexed with Fe^{2+}. When receptor1 is complexed with Fe^{2+} ion, none of the interfering metal ions examined showed any evident interference (Fig. 2). This result implies that receptor1 could be used for the selective detection of Fe^{2+} ion in various applications.

Binding and stoichiometry studies

To find the binding ability of receptor1 with Fe^{2+} ion, the fluorescence study was carried out by gently increasing the concentration of Fe^{2+} ion from 0 to 85 equivalents. A decrease in fluorescence intensity was observed with an increase in Fe^{2+} ion concentration (Fig. 3). The fluorescence intensity was almost saturated upon the addition of 85 equivalents of Fe^{2+}. The binding ratio of ligand and complex was predicted by Job's plot. The Job's plot

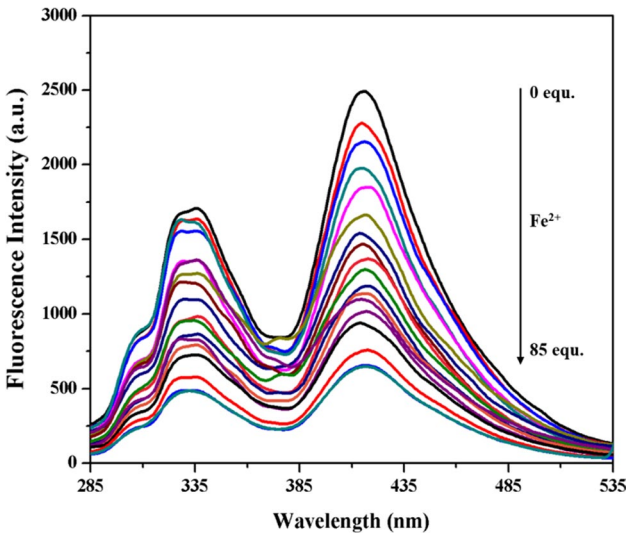

Fig. 3 Fluorescence titration spectrum of receptor1 (4×10^{-6} M) solution (DMF–H_2O, 1:1 v/v, HEPES 50 mM, pH = 7.4) upon addition of different concentration of $Fe.^{2+}$ (0–85 equivalents. λ_{ex} = 275 nm)

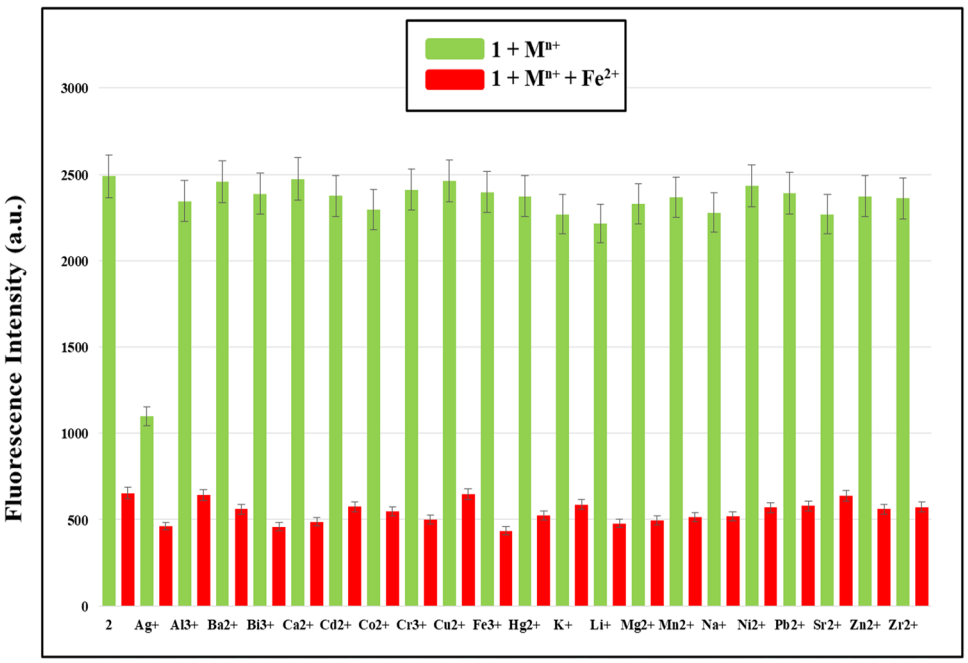

Fig. 2 Metal ions competition analysis of receptor1 (4×10^{-6} M) solution (DMF–H_2O, 1:1 v/v, HEPES = 50 mM, pH = 7.4) in the presence of various metal ions (100 equivalents. of each, λ_{ex} = 275 nm). The green bar represents the receptor1 + metal ion and the red bar represents receptor1 + metal ion + Fe^{2+} ion that shows the quenching fluorescence intensity

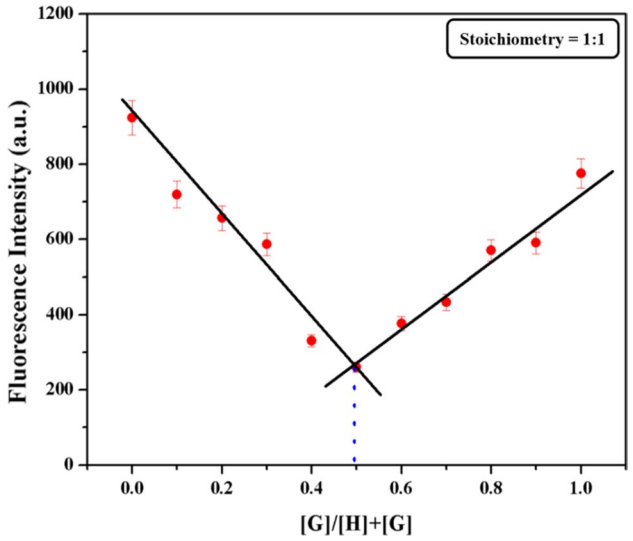

Fig. 4 Job's plot of receptor1 and Fe.$^{2+}$ in DMF–H_2O solution (1:1 v/v, HEPES 50 mM, pH = 7.4)

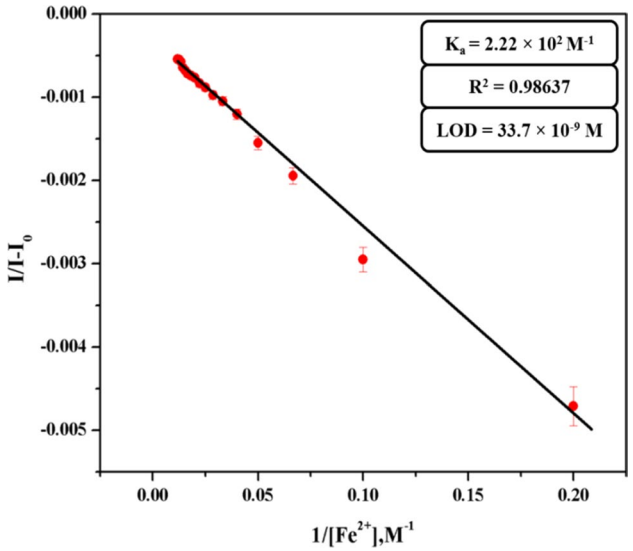

Fig. 5 Benesi–Hildebrand plot of receptor1 (4 μM) with Fe.$^{2+}$ in DMF–H_2O solution (1:1 v/v, HEPES 50 mM, pH = 7.4) (λ_{ex} = 275 nm)

confirms the binding mode of the host–guest complex, the maximum mole fraction of the complex was 0.5 at excitation wavelength 275 nm (Fig. 4). Job's plot concludes that the receptor1 interacts with Fe^{2+} at 1:1 stoichiometry. The stoichiometry binding of receptor and metal was predicted theoretically with the help of the Benesi–Hildebrand nonlinear fitting curve (Fig. 5) (Velmurugan 2014; Prabhu 2015a; Velmurgan 2015). The association constant (K_a) of receptor1–Fe^{2+} ion is 2.22×10^2 M^{-1}. The limit of detection (LOD) calculated using 3δ/S is 33.7×10^{-9} M, where δ denotes the standard deviation of the free probe, and S denotes the slope of the linear calibration plot indicating correlation coefficient (R^2) value of 0.9863 derived from the linear graph plot (Fig. 5). Imidazole, tripodal, tris-salicylidene (2-aminoethyl) amine, naphthalene, oxadiazole-based chemosensor results in detection of Fe^{2+} ion at the concentration of 0.32, 1.09, 1.3, 0.0048, 7.78 μM, respectively (Table 1), but in the present study receptor1 was able to detect the Fe^{2+} ion at the concentration of 0.003 μM which is very low compared to other Schiff-based compound.

Reversibility studies

The reversible characteristic of the synthesized chemosensor makes it suitable for a variety of applications. Using the chelating chemical EDTA, the reversible property of receptor1 is investigated (ethylenediaminetetraacetic acid). Figure 6a represents receptor1's reversible property. For receptor1, the fluorescence intensity is enhanced. The fluorescence intensity is lowered due to receptor1 complexation with the Fe^{2+} ion, by the addition of Fe^{2+} ion to the receptor1. The fluorescence intensity is also increased when EDTA is added to receptor1 and Fe^{2+} ion solution. This research demonstrates receptor1's excellent reversibility. The repeatability of the reversible property is further demonstrated by the addition of Fe^{2+} ion and EDTA multiple times. The complexation of EDTA and Fe^{2+} ions with receptor1 causes the intensity of Fe^{2+} and EDTA to vary. The cycle was repeated a total of ten times (Fig. 6b).

Table 1 Literature reports of other Schiff's-based compound sensing Fe^{2+} ion

Receptor Type	Mode of detection	Testing media	Binding constant Ka(M^{-1})	Limit of detection	References
Imidazole-based	Turn-Off	Bis–tris buffer	1.4×10^4	0.32 μM	Tae Geun Jo et al.
Tripodal-based	Turn-Off	Methanol: Water	2.49×10^4	1.09 μM	Atikal Farhi et al.
Tris salicylidene(2-aminoethyl)amine based	Turn-On	HEPES/Methanol	4.30	1.3 μM	Kyung Beom Kim et al.
Naphthalene based	Turn-Off	HEPES/Water	1.91×10^5	0.0048 μM	Bhuvanesh et al.
Oxadiazole based	Turn-Off	THF/Water(1:1)	4859.54	7.78 μM	Xue Gong et al.

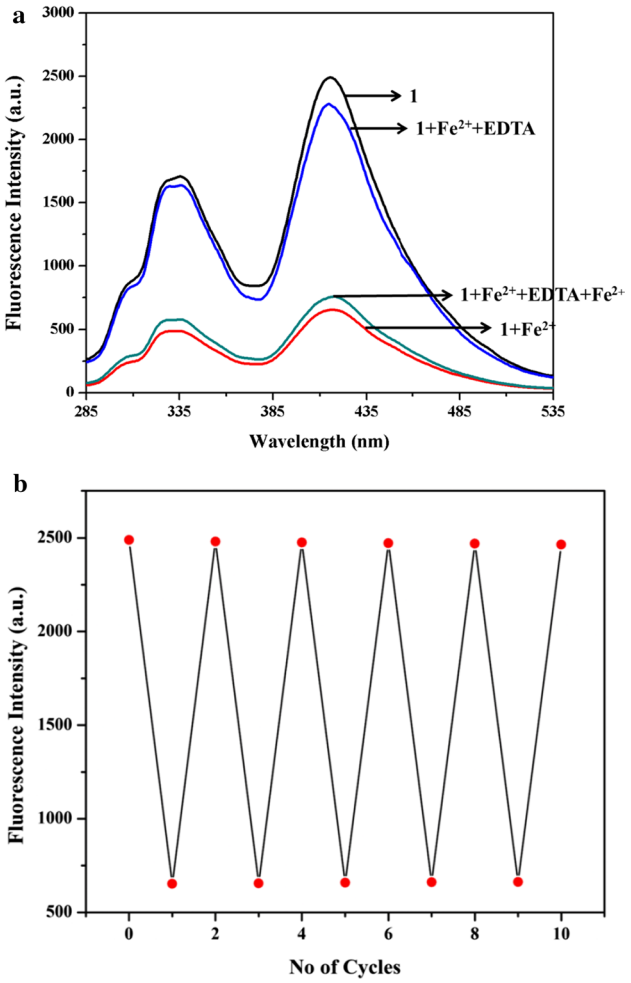

Fig. 6 **a** Reversibility spectra of receptor1 in the presence of Fe^{2+} ion and EDTA in DMF–H_2O solution (1:1 v/v, HEPES 50 mM, pH = 7.4) (λ_{ex} = 275 nm). **b** Sequential addition of Fe^{2+} and EDTA showing reversibility behavior

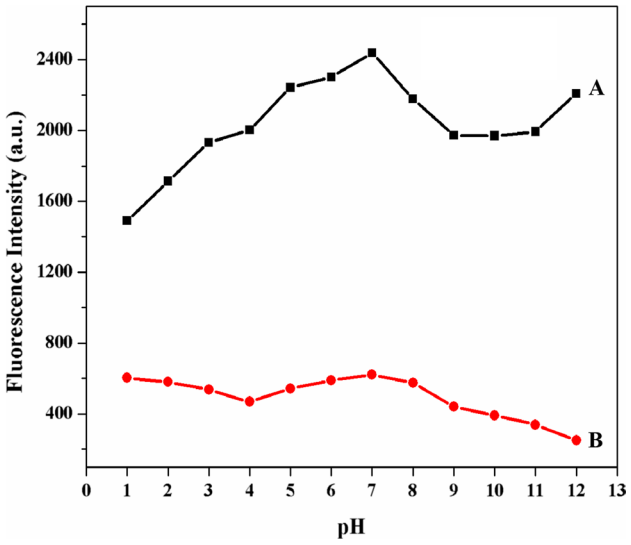

Fig. 7 Change in fluorescence intensity of A) Receptor1 B) Receptor1–Fe^{2+} with respect to pH

Effect of pH and time

The pH investigation is conducted to determine the synthesized receptor1's ability to function under various environmental conditions. Adjusting the pH from acidic to basic (2–11) conditions has a consequence on the receptor1 and receptor1–Fe^{2+} complex. In acidic pH, the fluorescence intensity of the receptor1–Fe^{2+} complex falls, increases at neutral pH, and then decreases again at basic pH (Fig. 7). The decrease in fluorescence intensity at acidic pH is because the imine (C=N) group of receptor1 gets protonated due to the increase in H^+ ion concentration and cleavage may take place between the fluorophore and the heterocyclic group hindering the binding of Fe^{2+} ion with receptor1 (Li et al. 2006). On the other hand, even under the basic condition, the fluorescence intensity decreases. This is because of the deprotonation of H^+ ion from a phenolic group of fluorophore due to the increase in the concentration of ^-OH ion. After deprotonation, the Na^+ ion occupies the phenoxide group and results in O^-Na^+ which hinders the binding of Fe^{2+} ion with receptor1 leading to a decrease in fluorescence intensity. The change in fluorescence intensity at acidic and basic conditions is due to the presence of the fluorophore group in receptor1. The increased fluorescence intensity at 7.4 indicates that the receptor1 works at physiological pH of 7.4 which is suitable for biological and environmental application. Hence, all the other experiments are carried out at pH 7.4.

A study was carried out further to assess the time taken for the complex formation between receptor1 and Fe^{2+} (Kumar et al. 2018). The decrease in fluorescence intensity

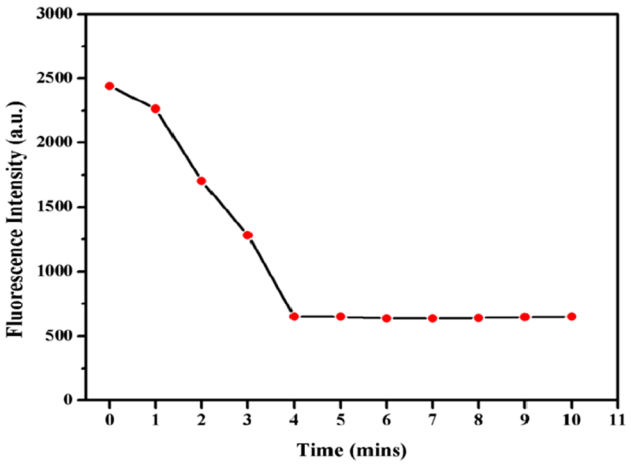

Fig. 8 Time taken for the complexation of receptor1–Fe.$^{2+}$ in DMF–H_2O solution (1:1 v/v, HEPES 50 mM, pH = 7.4) (λ_{ex} = 275 nm)

Table 2 Fe^{2+} ion recovered from real water sample spiked with Fe^{2+} ion using receptor1

CIT Water Sample	Fe^{2+} added (μM)	Fe^{2+} analyzed from fluorescence spectra (μM) mean[a] ± SD[b]	Recovery (%)	Relative error (%)
Borewell water 1	3.0	2.88 ± 0.15	96.0	– 4.0
Borewell water 2	6.0	5.96 ± 0.05	99.3	– 0.7
Tap water 1	3.0	3.02 ± 0.05	100.7	0.7
Tap water 2	6.0	5.93 ± 0.03	98.8	– 1.2
RO drinking water 1	3.0	3.04 ± 0.14	101.3	1.3
RO drinking water 2	6.0	5.97 ± 0.06	99.5	– 0.5

[a]Mean of three measurement

[b]Standard deviation

from 0 to 4th minute showed that the complexation between receptor1 and Fe^{2+} ion was unstable. After the 4th minute, the saturation in the graph indicates the stable complexation between receptor1 and Fe^{2+} ion. The solution was kept further for 60 minutes and the fluorescence intensity was noted. There were no desirable changes after four minutes (Fig. 8). Hence, the result shows that receptor1 favors for detection of Fe^{2+} ion in a short interval of time.

Application studies

Determination of Fe^{2+} ion in water sample

The synthesized receptor1 was subjected to the detection of Fe^{2+} ion in the water sample. Three different water samples (Bore well water (B1–3 , B2–6 μM), tap water (T1–3 , T2–6 μM), and RO drinking water (D1–3 , D2–6 μM)) are collected from Coimbatore Institute of Technology. The sample water is spiked with Fe^{2+} ion concentrations of 3 and 6 μM**.** About 2 mL of 4×10^{-6} M concentration of receptor1 was added to the spiked water sample. The recovery percentage of Fe^{2+} ion from spiked water sample after adding receptor1 is calculated from fluorescence spectroscopy (Fig. S4). The receptor1 showed the enhanced fluorescence intensity, but on adding the spiked water sample with receptor1, the quenching in fluorescence intensity is noticed. The difference in the fluorescence intensity is due to the complexation of Fe^{2+} ion with receptor1. The quenching in intensity proves that the receptor1 can attract Fe^{2+} ion from the spiked water sample. The recovery percentage of Fe^{2+} ion for B1, B2 is 96, 99.3%, for T1, T2 is 100.7, 98.8%, and for D1, D2 is 101.3, 99.5%, respectively (Table 2). The results proved that receptor1 could be practically applicable for selective detection of Fe^{2+} ion in real water sample analysis.

Molecular logic gate

Simple molecular structures combinational molecular gates can be created by combining Boolean logic gates, allowing a single molecule to conduct complex processes. Combinational molecular logic gates shown in the literature are used as a molecular calculator that performs distinct arithmetic operations such as addition and subtraction; as a molecular keypad lock for information security; and as a fluorescence sensor for the detection of multiple metal ions. We presented an easy sequential molecular logic circuit in the form of a binary logic circuit for molecular level information processing that demonstrates the 'Writing-Reading-Erasing-Reading' way (Cakmak 2018; Zong 2009). The excellent reversible property of receptor1 helped to construct a molecular logic gate using two binary inputs. The absence and presence of Fe^{2+} and EDTA were represented by '0' and '1' (i.e., presence of Fe^{2+} and EDTA as 1 and the absence of Fe^{2+} and EDTA as 0). The output is monitored at 420 nm. Based on the change in fluorescence intensity, the truth table was constructed. The output '0' denotes the quenching intensity (fluorescence-off) and '1' denotes the enhanced intensity (fluorescence-on). Based on the truth table, the INHIBIT logic gate was constructed as shown in Fig. 9. Thus, the

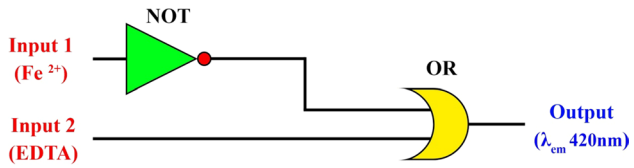

Fig. 9 INHIBIT molecular logic gate of 2-aminothiazolesalicylaldehyde (receptor1)

Table 3 Truth table of INHIBIT logic gate (λ_{em}- emission wavelength)

Input 1 (Fe^{2+})	Input 2 (EDTA)	Output (λem 420 nm)
0	0	1
1	0	0
0	1	1
1	1	1

addition of Fe^{2+} to receptor1 shows the weak fluorescence and on adding EDTA to receptor1–Fe^{2+} complex the fluorescence intensity is enhanced (Table 3).

Molecular keypad lock

At the molecular level, the combinational logic gate is used for the imitation of variety of electronic devices. The main goal is to create new information processing pattern, by pushing over silicon-based technology which could result in electronic devices with compactness, power usage and efficiency. It is currently possible to integrate various imitating electrical components, such as comparators, memory units, and DE multiplexers. The recent application of molecular logic gate showed the mimicking behavior. A major electrical logic device, the keypad lock, has recently been molecularly replicated. This technology can be used in a variety of circumstances wherein admission to an object or information is limited to a small group of persons who know the valid password to open the keypad lock. The fundamental advantage of a keypad lock system over a simple logic gate is that its output signals are dependent not only on the right element of a sequence but also on the order in which they are delivered. As a result, a molecular device construction authorizing password entry is an extremely intriguing research goal because it represents a novel approach of safeguarding information at the molecular level (Wang et al. 2011). The excellent reversible property helped us to propose a sequence of code for the molecular keypad to lock. Three different chemical input was given as receptor1 'R,' Fe^{2+} metal ion 'F,' and EDTA 'E.' The six feasible input fusions are RFE, REF, FRE, FER, ERF, and EFR. In these combinations, RFE resulted in enhanced fluorogenic output, whereas the other combination such as REF, FRE, FER, ERF, and EFR results in quenching intensity as output as shown in Fig. 10. The keypad contains the alphabet from A to Z, and the password RFE unlocks the keypad. At the same time, the other codes result in the wrong password. Due to this reason, this type of sensing will safeguard molecular-level information.

Molecular docking studies

Molecular docking has been shown in several studies to be a valuable tool for analyzing the interaction of a protein receptor with its ligand and disclosing its binding mechanism. In this study, flexible docking techniques were used to find the best ligand. Binding sites have been found in the target proteins (Subhasri et al. 2014). Here, the structure-based receptor1 bound with NUDT5 could inhibit the activity of NUDT5 and thereby inhibit the proliferation of breast cancer cells. NUDT5 is a nucleotide metabolizing enzyme linked with ADP ribose and 8-oxoguanine metabolism. NUDT5 influences the hormones that regulate the gene pool and increases the breast cancer cells. The synthesized receptor1 acts as a ligand and it is subjected to molecular docking using Schrodinger Maestro software to assess its interactions with the protein. The performance of receptor1 was high when it is docked with NUDT5, a macromolecule that acts as a silence hormone signaling in breast cancer (PDB IB: 5NWH) (Sultana et al. 2019). In NUDT5, the aminoacid residues implicated in binding pockets are so predicted with the ligand molecule. Nine potential binding sites of NUDT5 involved in interaction with receptor1 are ILE 141, TRP 28, ARG 51, ALA 96, VAL 29, GLY 97, LEU 98, MET 132, and CYS 139 (Fig. S4). As a result, all of these binding pockets were confirmed to be significant and were used to generate the docking grid. The receptor1 binds with ASP 274 through hydrogen bonding at the ortho-position of the receptor1 moiety. The receptor1 has electrostatic interaction with LEU 178, VAL 174, LEU 169, LEU 164, PHE

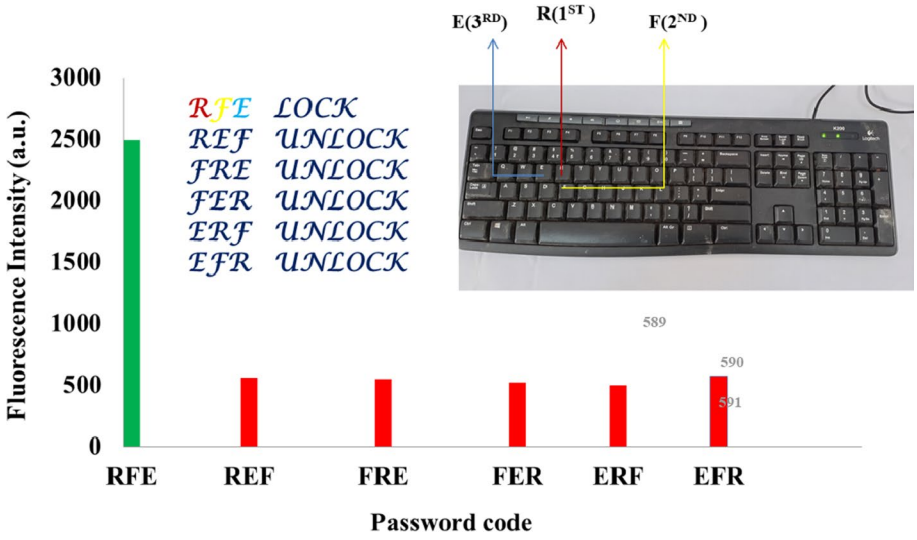

Fig. 10 Output for recepor1, corresponding to six possible input combinations of receptor1 series at 420 nm. Inset: a molecular keypad lock generating emission at 420 nm at correct password RFE entered. The keys R, F, and E hold the relevant input receptor1, Fe^{2+}, and EDTA, respectively

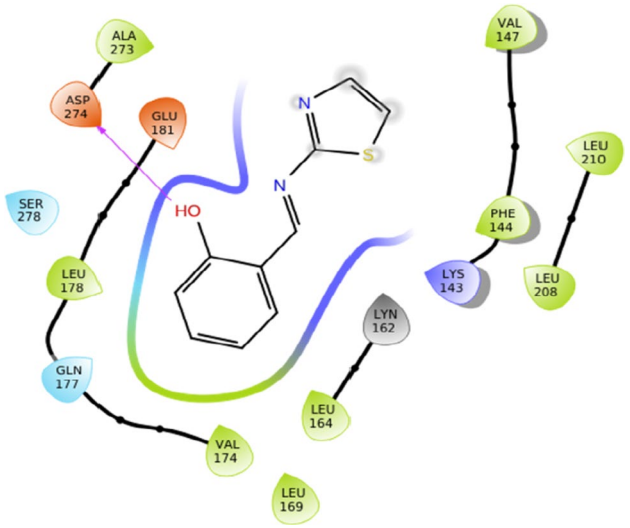

Fig. 11 2D Binding activity of receptor1 with NUDT5

144, VAL 147, LEU 210, LEU 208, and ALA 273, as well as it has a polar contact with ASP 274. The phenyl group of receptor1 appears to create a parallel, π–π stacked configuration, according to the molecular docking model (Fig. 11). The docking score of electrostatic interaction between receptor1 and protein is -5.23 kcal mol^{-1}. The docking score of net negative energy represents a stable complex. The binding phenomenon is due to existence of heteroatoms, asymmetric charge distribution over the receptor and electrostatic interactions. The docking result indicates that the receptor1 has shown good affinity toward NUDT5 target. Thus, receptor1 may act as an inhibitor for blocking NUDT5 activity.

Advantages over other methods

The adopted fluorescence method for the determination of iron is compared with the other reported methods (Table 4). From the table, it is inferred that the LOD and time for detection are superior in the proposed work compared to other reported methods (Andrea 2012, Alikhani et al. 2017, Xin 2009, Taeuk 2017, Ugo 2002). The accessibility, quickness, inexpensive, and specific detection are the other advantages of the proposed method.

Conclusion

A Schiff base receptor1 is synthesized using salicylaldehyde and thiazole moieties. The receptor1 is highly selective toward Fe^{2+} ion showing quenching with turn off–on process following reverse PET mechanism. The receptor1 selectively and preferentially binds with Fe^{2+} ion among other competitive metal ion. The association constant of receptor1–Fe^{2+} ion is $2.22 \times 10^{2\ M-1}$ and limit of detection (LOD) is 33.7×10^{-9} M. The receptor1 detect Fe^{2+} ion at a very low concentration of 0.003 µM, which is lower than the EPA's drinking water limits of 5.37 µM. The binding ratio of receptor1–Fe^{2+} is proposed to be 1:1 by Job's plot. The receptor1–Fe^{2+} ion is found to be reversible with EDTA solution. Based on this property, a molecular logic gate is constructed with two inputs and one output and this type of receptor1 can be successfully applied for the mimicking behavior of molecular keypad lock which is highly utilized in security devices. The receptor1 is applied in real time for detecting Fe^{2+} ion in water samples and in molecular docking study. The Fe^{2+} ion recovery percentages for (Bore Water) B1, B2 are 96 and 99.3%, respectively, for (tap water) T1, T2 is 100.7 and 98.8% and for (drinking water) D1, D2 is 101% and 99.5%. Receptor1 docks with NUDT5, a hormone signaling a breast cancer cell, show the good docking score of – 5.23 kcal mol^{-1}. To conclude, a new selective fluorescent receptor1 (2-aminothiazolesalicylaldehyde) is a good candidate which could be used for both biological and environmental system.

Table 4 Comparison of the current work for determination of Fe^{2+} with other reported methods

ReferenceS	Detection of metal	Detection method	Solvent	Limit of detection	Time (min)
Andrea Spoalaor et al.	Fe^{2+}	ICP-MS	–	0.01 ng mL^{-1}	shorter
Amench AliKhani et al.	Fe^{2+}	Flame atomic absorption	Methanol:$CHCl_3$	5.6 µg L^{-1}	< 1
Xin Jin et al.	Fe^{2+}	Electrochemical	–	0.02 mM	–
Taeuk An et al.	Fe^{2+}	Magnetic resonance imaging	Distilled water	–	4.26
Ugo et al.	Fe^{2+}	Potentiometry	–	–	10
Present work	Fe^{2+}	Fluorometric	DMF–H_2O	0.0033 µM	< 4

Supplementary Information The online version contains supplementary material available at https://doi.org/10.1007/s11696-022-02373-z.

Acknowledgements Authors Summaya Banu Basha and Hemalatha Kuzhandaivel would like to thank the Technical Education and Quality Improvement Programme, Phase-III (TEQIP-III), for the financial assistance and facilities to carry out this research work. Also, we thank the management and principal of Coimbatore Institute of Technology (CIT) for their constant encouragement and support. Immanuel David Charles and Nandhakumar Raju would like to thank SERB-EMR grant by the DST (Sanction No. *SERB-EMR/2016/005692*) at KITS.

Funding This research is supported by TEQIP III (Technical Education Quality Improvement Programme III) for providing the instrumentation facilities to undertake this research. This work is also supported by the SERB-EMR grant by the DST (Sanction No. *SERB-EMR/2016/005692*) at KITS.

I hereby declare that this is the original work done by the stated authors and has not been submitted elsewhere for publication.

Declarations

Conflict of interest There are no competing interests.

References

Ahmed MJ, Islam MT, Nime M (2015) A highly selective and sensitive spectrophotometric method for the determination of selenium using 2-hydroxy-1-napthaldehyde orthoaminophenol. Anal Methods 7(18):7811–7823. https://doi.org/10.1039/c5ay01311a

Alikhani A, Eftekhari M, Chamsaz M, Gheibi M (2017) Paired-ion-based liquid phase microextraction for speciation of iron (Fe^{2+}, Fe^{3+}) followed by flame atomic absorption spectrometry. J Food Measure Characterization: https://doi.org/10.1007/s11694-017-9669-0

Andrea S, Paul V, Jacopo G, Giulio C, Claude B, Carlo B (2012) Determination of Fe^{2+} and Fe^{3+} species by FIA-CRC-ICP-MS in Antarctic ice samples. J Anal Spectrom 27(2):656. https://doi.org/10.1039/c1ja10276a

Asiri AM, Al-Ghamdi NSM, Kumar P, Khan SA (2019) Physicochemical and Photophysical investigation of newly synthesized carbazole containing pyrazoline-benzothiazole as fluorescent chemosensor for the detection of $Cu^{2+,}$ Fe^{3+} and Fe^{2+} metal ion. J Mol Struct 1195:670–680. https://doi.org/10.1016/j.molstruc.2019.05.088

Balasubramanian M, Adaikalam S, Sundarave VK, Stephen R, Raju RK (2020) Thiazole-tethered biaryls as fluorescent chemosensors for the selective detection of Fe^{3+} Ions. J Heterocyclic Chem. https://doi.org/10.1002/jhet.4093

Bhuvanesh N, Velmurugan K, Suresh S, Prakash P, John N, Murugan-Nandhakumar SR (2017) Naphthalene based fluorescent chemosensor for Fe^{2+} ion detection in microbes and real water samples. J Lumin 188:217–222. https://doi.org/10.1016/j.jlumin.2017.04.026

Cakmak SE, Kolemen S, Sedgwick AC, Gunnlaugsson T, James TD, Yoon J, Akkaya EU (2018) Molecular logic gates: the past, present and future. Chem Soc Rev 47:2228–2248. https://doi.org/10.1039/c7cs00491e

Chae JB, Yun D, Lee H, Lee H, Kim KT, Kim C (2019) Highly sensitive dansyl-based chemosensor for detection of Cu^{2+} in aqueous solution and zebrafish. ACS Omega 4(7):12537–12543. https://doi.org/10.1021/acsomega.9b00970

Chereddy NR, Thennarasu S, Mandal AB (2013) A highly selective and efficient single molecular FRET based sensor for ratiometric detection of Fe^{3+} ions. Analyst 138:1334–1337. https://doi.org/10.1039/c3an36577h

Das S, Dutta M, Das D (2013) Fluorescent probes for selective determination of trace level Al^{3+}: recent developments and future prospects. Anal Methods 5(22):6262. https://doi.org/10.1039/c3ay40982a

Dong L, Wu C, Zeng X, Mu L, Xue SF, Tao Z, Zhang JX (2010) The synthesis of a rhodamine B schiff-base chemosensor and recognition properties for Fe^{3+} in neutral ethanol aqueous solution. Sens Actuators B 145:433–437. https://doi.org/10.1016/j.snb.2009.12.057

Fan L, Li T, Wang B, Yang Z, Liu C (2014) A colorimetric and turn-on fluorescent chemosensor for Al(III) based on a chromone Schiff-base. Spectrochim Acta-a 118:760–764. https://doi.org/10.1016/j.saa.2013.09.062

Farhi A, Firdaus F, Shakir M (2018) Design and application of tripodal on-off type chemosensor for discriminative and selective detection of Fe^{2+} ions. New J Chem. https://doi.org/10.1039/C8NJ00214B

Gholami M, Rezayi M, Nia PM, Yusoff I, Alias Y (2015) A novel method for fabricating Fe^{2+} ion selective sensor using polypyrrole and sodium dodecyl sulfate based on carbon screen-printed electrode. Measurement 69:115–125. https://doi.org/10.1016/j.measurement.2015.03.030

Golbedaghi R, Alavipour E, Shahsavari M (2018) Salicylaldehyde-based 'turn-off' fluorescent chemosensor with high selectivity for Fe^{3+} in H2O-DMF solution. Russian J Inorg Chem 63:414–419. https://doi.org/10.1134/S003602361803019

Gong X, Zhang H, Jiang N, Wang L, Guang, (2019) Oxadiazole-based "on-off" fluorescence chemosensor for rapid recognition and detection of Fe^{2+} and Fe^{3+} in aqueous solution and in living cells. Microchem J 145:435–443. https://doi.org/10.1016/j.microc.2018.11.011

Gou C, Qin SH, Wu HQ, Wang Y, Luo J, Liu XY (2011) A highly selective chemosensor for Cu^{2+} and Al^{3+} in two different ways based on Salicylaldehyde Schiff. Inorg Chem Commun 14(10):1622–1625. https://doi.org/10.1016/j.inoche.2011.06.024

Huang L, Hou F, Cheng J, Xi P, Chen F, Bai D, Zeng Z (2012) Selective off–on fluorescent chemosensor for detection of Fe^{3+} ions in aqueous media. Org Biomol Chem 10(48):9634. https://doi.org/10.1039/c2ob26258d

Jo TG, Jung JM, Han J, Lim MH, Kim C (2013) A single fluorescent chemosensor for multiple targets of $Cu^{2+,}$ $Fe^{2+/3+}$ and Al^{3+} in living cells and a near-perfect aqueous solution. Dyes Pigments 99:661–665. https://doi.org/10.1039/c7ra05565j

Jo TG, Bok KH, Han J, Lim MH, Kim C (2017) Colorimetric detection of Fe^{3+} and Fe^{2+} and sequential fluorescent detection of Al^{3+} and pyrophosphate by an imidazole-based chemosensor in a near-perfect aqueous solution. Dyes Pigments 139:136–147. https://doi.org/10.1016/j.dyepig.2016.11.052

Joeseph R, Chinta JP, Rao CP (2011) Calix[4]arene-Based 1,3-Diconjugate of Salicylyl Imine Having Dibenzyl amine moiety (L): synthesis, characterization, receptor Properties toward Fe^{2+}, Cu^{2+}, and Zn^{2+}, crystal structures of Its Zn^{2+} and Cu^{2+} complexes, and selective phosphate sensing by the [ZnL]. Inorg Chem 50:7050–7058. https://doi.org/10.1021/ic200544a

Khairnar N, Tayade KC, Sahoo SK, Bondhopadhyay B, Basu A, Singh J, Singh N, Gite VV, Kuwar A (2015) A highly selective fluorescent 'turn-on' chemosensor for Zn^{2+} based on a benzothiozole conjugate, their applicable in live cell imaging and resultant complex as secondary sensor of CN^{-}. Dalton Trans 44(5):2097–2102. https://doi.org/10.1039/C4DT03247K

Khan SA, Ullah Q, Almalki ASA, Kumar S, Obaid RJ, Alsharif MA, Hashmi AA (2021) Synthesis and photophysical investigation of

(BTHN) Schiff base as off-on Cd^{2+} fluorescent chemosensor and its live cell imaging. J Mol Liq 328:115407. https://doi.org/10.1016/j.molliq.2021.115407

Kim KB, Kim H, Song EJ, Kim S, No I, Kim C (2013) A cap-type Schiff base acting as a fluorescence sensor for zinc(II) and a colorimetric sensor for iron(II), copper(II), and zinc(II) in aqueous media. Dalton Trans 42:16569–16577. https://doi.org/10.1039/c3dt51916c

Kim S, Lee H, Chae JB, Kim C (2020) A pyrene-mercapto-based probe for detecting Ag^{+} by fluorescence turn-on. Inorg Chem Commun. https://doi.org/10.1016/j.inoche.2020.108044

Kumar M, Kumar A, Faizi MSH, Kumar S, Singh MK, Sahu SK, John RP (2018) A selective "turn-on" fluorescent chemosensor for detection of Al^{3+} in aqueous medium: Experimental and theoretical studies. Sensor Actuat B Chem 260:888–899. https://doi.org/10.1016/j.snb.2018.01.098

Kumar R, Ravi S, Immanuel David C, Nandhakumar R (2020) A photo-induced electron transfer based reversible fluorescent chemosensor for specific detection of Mercury (II) ions and its applications in logic gate, keypad lock and real samples. Arabian J Chem. https://doi.org/10.1016/j.arabjc.2020.11.017

Lee JA, Eom GH, Park HM, Lee JH, Song H, Hong CS (2012) Selective Fe^{2+} Ion recognition using a fluorescent pyridinyl-benzo imidazole-derived Ionophore. Bull Korean Chem Soc 33:3625–3628. https://doi.org/10.5012/bkcs.2012.33.11.3625

Li J, Li J (2018) A luminescent porous metal–organic framework with Lewis basic pyridyl sites as a fluorescent chemosensor for TNP detection. Inorg Chem Commun 89:51–54. https://doi.org/10.1016/j.inoche.2018.01.013

Li CY, Zhang XB, Jin Z, Han R, Shen GL, Yu RQ (2006) A fluorescent chemosensor for cobalt ions based on a multi-substituted phenol-ruthenium(II) tris(bipyridine) complex. Analytica Chim Acta 580(2):143–148. https://doi.org/10.1016/j.aca.2006.07.054

Li N, Tang W, Xiang Y, Tong A, Jin P, Ju Y (2010) Fluorescent salicylaldehyde hydrazone as selective chemosensor for Zn^{2+} in aqueous ethanol: a ratiometric approach. Luminescence 25(6):445–451. https://doi.org/10.1002/bio.1175

Li J, Wang Q, Guo Z, Ma H, Zhang Y, Wang B, Bin D, Wei Q (2016) Highly selective fluorescent chemosensor for detection of Fe^{3+} based on Fe3O4@ZnO. Sci Rep 6:23558. https://doi.org/10.1038/srep23558

Luo A, Wang H, Wang Y, Huang Q, Zhang Q (2016) A novel colorimetric and turn-on fluorescent chemosensor for iron(III) ion detection and its application to cellular imaging. Spectrochim Acta Part A Mol Biomol Spectrosc 168:37–44. https://doi.org/10.1016/j.saa.2016.05.048

Moon KS, Yang YK, Ji SH, Tae JS (2010) Aminoxy-linked rhodamine hydroxamate as fluorescent chemosensor for Fe^{3+} in aqueous media. Tetrahedron Lett 51:3290–3293. https://doi.org/10.1016/j.tetlet.2010.04.068

Murugan AS, Vidhyalakshmi N, Ramesh U, Annaraj J (2018) In vivo bio-imaging studies of highly selective, sensitive rhodamine based fluorescent chemosensor for the detection of Cu^{2+}/Fe^{3+} ions. Sensor Actuat B-Chem 274:22–29. https://doi.org/10.1016/j.snb.2018.07.104

Nagarajan R, Ryoo HI, Vanjare BD, Gyu CN, Hwan LK (2021) Novel phenylalanine derivative-based turn-off fluorescent chemosensor for selective Cu^{2+} detection in physiological pH. J Photochem Photobiol, A 418:113435. https://doi.org/10.1016/j.jphotochem.2021.113435

NuriKurunlu A (2015) A fluorescent "turn on" chemosensor based on Bodipy–anthraquinone for Al(III) ions: synthesis and complexation/spectroscopic studies. RSC Adv 5(51):41025–41032. https://doi.org/10.1039/c5ra03342j

Prabhu J, Velmurugan K, Nandhakumar R (2015a) Pb^{2+} ion induced self-assembly of anthracene based chalcone with a fluorescence turn on process in aqueous media. J Anal Chem 70(8):943–948. https://doi.org/10.1134/S1061934815080134

Prabhu J, Velmurugan K, Nandhakumar R (2015b) Development of fluorescent lead II sensor based on an anthracene derived chalcone. Spectrochim Acta Part A 144:23. https://doi.org/10.1016/j.saa.2015.02.028

Saravanan A, Shyamsivappan S, Suresh T, Subashini G, Kadirvelu K, Bhuvanesh N, Nandhakumar R, Mohan PS (2019) An efficient new dual fluorescent pyrene based chemosensor for the detection of bismuth (III) and aluminium (III) ions and its applications in bio-imaging. Talanta. https://doi.org/10.1016/j.talanta.2019.01.114

Sen S, Sarkar S, Chattopadhyay B, Moirangthem A, Basu A, Dhara K, Chattopadhyay P (2012) A ratiometric fluorescent chemosensor for iron: discrimination of Fe^{2+} and Fe^{3+} and living cell application. Analyst 137(14):3335. https://doi.org/10.1039/c2an35258c

Subhasri A, Anbuselvan C, Rajendraprasad N (2014) Twin applications of highly selective Cu^{2+} fluorescent chemosensor and cytotoxicity of 2-(2-phenylhydrazono)-1H-indene-1,3(2H)-dione and 2-(2-(4-methoxyphenyl)hydrazono)-1H-indene-1,3(2H)-dione: molecular docking and DFT Studies. Rsc Adv 4(105):60658–60669. https://doi.org/10.1039/C4RA11006D

Sultana R, Islam M, Haque MA, Evamoni FZ, Imran ZM, Khanom J, Munim MA (2019) Molecular docking based virtual screening of the breast cancer target NUDT5. Biomed Inf 15(11):784–789. https://doi.org/10.6026/97320630015784

Suresh S, Bhuvanesh N, Prabhu J, Thamilselvan A, Rajkumar SRJ, Kannan K, Kannan VR, Nandhakumar R (2018) Pyrene based chalcone as a reversible fluorescent chemosensor for Al^{3+} ion and its biological applications. J Photochem Photobiol A 359:172–182. https://doi.org/10.1016/j.jphotochem.2018.04.009

Taeuk A, Namhun L, Hong-Jun C, Seongsoo K, Dong-Sik S, Sang-Myung L (2017) Ultra-selective detection of Fe^{2+} ion by redox mechanism based on fluorescent polymerized dopamine derivatives. RSC Adv 7:30582. https://doi.org/10.1039/c7ra04107a

Tamil Selvan G, Chitra V, Tamil Selvan R, Israel Enoch VMV, Mosae Selvakumar P (2018) On/Off fluorescent chemosensor for selective detection of divalent iron and copper ions: molecular logic operation and protein binding. ACS Omega 3(7):7985–7992. https://doi.org/10.1021/acsomega.8b00748

Ugo P, Moretto LM, Boni AD, Scopece P, Mazzocchin GA (2002) Iron(II) and iron(III) determination by potentiometry and ion-exchange voltammetry at ionomer-coated electrodes. Anal Chim Acta 474(1–2):147–160. https://doi.org/10.1016/s0003-2670(02)01015-2

Velmurugan K, Prabhu J, Tang L, Chidambaram T, Noel M, Radhakrishnan S, Nandhakumar R (2014) A simple chalcone-based fluorescent chemosensor for the detection and removal of Fe^{3+} ions using a membrane separation method. Anal Methods 6:2883. https://doi.org/10.1039/c3ay42139b

Velmurugan K, Kumar SM, Kumar SS, Amudha S, Nandhakumar R (2015) Specific fluorescent sensing of aluminium using naphthalene benzimidazole derivative in aqueous media. Spectrochim Acta Part A 139:119. https://doi.org/10.1016/j.saa.2014.11.103

Wang Y, Huang Y, Li B, Zhang L, Song H, Jiang H, Gao J (2011) A cell compatible fluorescent chemosensor for Hg^{2+} based on a novel rhodamine derivative that works as a molecular keypad lock. RSC Adv 1(7):1294. https://doi.org/10.1039/c1ra00488c

Wang Y, Wang C, Xue S, Liang Q, Li Z, Xu S (2016) Highly selective and sensitive colorimetric and fluorescent chemosensor of Fe^{3+} and Cu^{2+} based on 2,3,3- trimethylnaphto[1,2-d] squaraine. RSC Adv 6:6540–6550. https://doi.org/10.1039/C5RA22530B

Xin J, Botte GG (2009) Electrochemical technique to measure Fe(II) and Fe(III) concentrations simultaneously. J Appl Electrochem 39(10):1709–1717. https://doi.org/10.1007/s10800-009-9864-8

Xu H, Ding H, Li G, Fan C, Liu G, Pu S (2017) A highly selective fluorescent chemosensor for Fe^{3+} based on a new diarylethene with a rhodamine 6G unit. Rsc Adv 7(47):29827–29834. https://doi.org/10.1039/c7ra04728b

Yin W, Cui H, Yang Z, Li C, She M, Li J, Zhao G, Shi Z, Yin B (2011) Facile synthesis and characterization of rhodamine-based colorimetric and "off–on" fluorescent chemosensor for Fe^{3+}. Sens Actuators B 157:675–680. https://doi.org/10.1016/j.snb.2011.04.072

Yoldas A, Algi F (2015) An Imidazo-phenanthroline scaffold enables both chromogenic Fe(II) and fluorogenic Zn(II) detection. Rsc Adv 5(11):7868–7873. https://doi.org/10.1039/C4RA14182B

Zhan J, Wen L, Miao F, Tian D, Zhu X, Li H (2012) Synthesis of a pyridyl-appended calix[4]arene and its application to the modification of silver nanoparticles as Fe^{3+} colorimetric sensor. New J Chem 36:656. https://doi.org/10.1039/c2nj20776a

Zhang Y, Cao X, Wu G, Wang J, Zhang T (2020) Quaternized salicylaldehyde Schiff base modified mesoporous silica for efficiently sensing Cu(II) ions and their removal from aqueous solution. Appl Surf Sci. https://doi.org/10.1016/j.apsusc.2020.146803

Zhou Z, Li N, Tong A (2011) A new coumarin-based fluorescence turn-on chemodosimeter for Cu^{2+} in water. Analytica Chim Acta 702(1):81–86. https://doi.org/10.1016/j.aca.2011.06.041

Zong G, Lu G (2009) An anthracene-based chemosensor for multiple logic operations at the molecular level. J Phys Chem C 113(6):2541–2546. https://doi.org/10.1021/jp8092379